Journal of Cerebral Blood Flow & Metabolism (2012) 32, 771–779

www.jcbfm.com

Feature Article

pH as a biomarker of neurodegeneration in Huntington's disease: a translational rodent-human MRS study

Myriam M Chaumeil[1,2], Julien Valette[1], Céline Baligand[2], Emmanuel Brouillet[1], Philippe Hantraye[1], Gilles Bloch[1], Véronique Gaura[1], Amandine Rialland[3], Pierre Krystkowiak[4], Christophe Verny[5], Philippe Damier[6], Philippe Remy[1,3], Anne-Catherine Bachoud-Levi[3,7,8], Pierre Carlier[2] and Vincent Lebon[1]

[1]*Commissariat à l'Energie Atomique, Institut d'Imagerie Biomédicale, Molecular Imaging Research Center, Centre National de la Recherche Scientifique, Unité de Recherche Associée, Fontenay-aux-Roses Cedex, France;* [2]*Institut de Myologie, Laboratoire de RMN, Paris, France;* [3]*Assistance Publique—Hôpitaux de Paris, Centre de Référence Maladie de Huntington, Hôpital Henri Mondor, Créteil, France;* [4]*Centre Hospitalier Régional Universitaire de Lille, Hôpital Roger Salengro, Lille, France;* [5]*Centre Hospitalier Universitaire d'Angers, Angers, France;* [6]*Centre Hospitalier Universitaire de Nantes, Hôpital Nord Laënnec, Nantes, France;* [7]*Institut National de la Santé et de la Recherche Médicale, Université Paris Est, Institut Mondor de Recherche Biomédicale, Créteil, France;* [8]*Département d'Etudes Cognitives, Ecole Normale Supérieure, Paris, France*

Early diagnosis and follow-up of neurodegenerative diseases are often hampered by the lack of reliable biomarkers. Neuroimaging techniques like magnetic resonance spectroscopy (MRS) offer promising tools to detect biochemical alterations at early stages of degeneration. Intracellular pH, which can be measured noninvasively by ^{31}P-MRS, has shown variations in several brain diseases. Our purpose has been to evaluate the potential of MRS-measured pH as a relevant biomarker of early degeneration in Huntington's disease (HD). We used a translational approach starting with a preclinical validation of our hypothesis before adapting the method to HD patients. ^{31}P-MRS-derived cerebral pH was first measured in rodents during chronic intoxication with 3-nitropropionic acid (3NP). A significant pH increase was observed early into the intoxication protocol (pH = 7.17 ± 0.02 after 3 days) as compared with preintoxication (pH = 7.08 ± 0.03). Furthermore, pH changes correlated with the 3NP-induced inhibition of succinate dehydrogenase and preceded striatum lesions. Using a similar MRS approach implemented on a clinical MRI, we then showed that cerebral pH was significantly higher in HD patients (n = 7) than in healthy controls (n = 6) (7.05 ± 0.03 versus 7.02 ± 0.01, respectively, P = 0.026). Altogether, both preclinical and human data strongly argue in favor of MRS-measured pH being a promising biomarker for diagnosis and follow-up of HD.
Journal of Cerebral Blood Flow & Metabolism (2012) **32,** 771–779; doi:10.1038/jcbfm.2012.15; published online 29 February 2012

Keywords: brain; Huntington's disease; pH; ^{31}P-MR spectroscopy; 3-nitropropionic acid

Introduction

Huntington's disease (HD) is a neurodegenerative disorder characterized by abnormal movements and dementia associated with degeneration of the striatum and to a lesser extent cerebral cortex (Brouillet *et al*, 2005; Harper, 1991). Even if mechanisms of neurodegeneration in HD remain partially unknown, defects in energy metabolism—in particular anomalies in succinate dehydrogenase (SDH) activity—might play a key role in the pathogenesis of this disorder (Beal, 2005; Brouillet *et al*, 1999; Damiano *et al*, 2010). This observation has driven numerous studies aiming at validating functional imaging measurements as biomarkers for HD. Positron emission tomography and magnetic resonance spectroscopy (MRS) studies have evidenced anomalies in cerebral glucose consumption (Kuhl *et al*, 1982; Powers *et al*, 2007), tricarboxylic acid (TCA) cycle rate (Boumezbeur *et al*, 2005; Henry *et al*, 2002), and concentrations of brain metabolites including lactate (Jenkins *et al*, 1998), *N*-acetylaspartate, and myo-inositol

Correspondence: Dr V Lebon, Commissariat à l'Energie Atomique, Institut d'Imagerie Biomédicale, Molecular Imaging Research Center, Centre National de la Recherche Scientifique, Unité de Recherche Associée, CEA—MIRCen, Bât. 61, 92265 Fontenay-aux-Roses Cedex, France.
E-mail: vincent.lebon@cea.fr
Received 25 July 2011; revised 24 October 2011; accepted 16 December 2011; published online 29 February 2012

(Dautry *et al*, 2000; Hoang *et al*, 1998), either in animal models or in patients. However, none of these measurements has proven sensitive and robust enough to serve as an early biomarker of HD, so that diagnosis and monitoring of the disease remain impossible before irreversible brain damage.

Among magnetic resonance approaches, ^{31}P-MRS has the advantage of detecting phosphorus-containing compounds, which are directly involved in cell energy metabolism, making it possible to assess the cerebral energetic status noninvasively. In particular, ^{31}P-MRS makes it possible to accurately assess the intracellular pH of living tissues (Petroff and Prichard, 1983). Magnetic resonance spectroscopy-measured pH anomalies have been reported in brain diseases such as epilepsy (van der Grond *et al*, 1998), brain tumor (Albers *et al*, 2005; Gerweck and Seetharaman, 1996), ischemia (Welch *et al*, 1992), chronic hypoxia (Hamilton *et al*, 2003), psychiatric disorders (Hamakawa *et al*, 2004; Jensen *et al*, 2008; Kato *et al*, 1994), and Parkinson's disease (Rango *et al*, 2006).

In this context, our aim was to test the hypothesis that cerebral pH is modified in HD using ^{31}P-MRS and therefore can be used as a biomarker of HD. The hypothesis was first validated in a well-characterized rat model of HD (Bizat *et al*, 2003*a*) using a 4-T preclinical MRI, demonstrating correlation of pH changes with brain SDH enzymatic activity. This approach was then translated to a clinical 3 T MRI to measure brain pH in a group of HD patients.

Materials and methods

Cerebral pH in a Rat Model of Huntington's Disease

3-Nitropropionic Acid Chronic Model of Huntington's Disease: This study was conducted on five male Lewis rats (336 ± 9 g, 12-week-old; Iffa Credo, L'Arbresle, France). All experimental procedures were performed in strict accordance with the recommendations of the European Community (86/609) and the French National Committee (87/848) for care and use of laboratory animals. A well-characterized model of chronic intoxication using 3-nitropropionic acid (3NP) was chosen (Bizat *et al*, 2003*a*): 3NP was delivered by continuous infusion at a dose of 54 mg/kg per day using osmotic minipumps (Alzet, Palo Alto, CA, USA) implanted subcutaneously in the back of the animals.

Localized ^{31}P Magnetic Resonance Spectroscopy and Magnetic Resonance Imaging in the Rat Brain: For all nuclear magnetic resonance experiments, animals were secured in the prone position in a custom-built cradle. A water-heating pad was used to keep body temperature stable. Anesthesia was induced with 5% isoflurane in a 1.5 ml/min oxygen flow and maintained with 2% isoflurane in a 1.5 ml/min oxygen flow applied with a face mask allowing free breathing. Rodent experiments were performed on a 4-T magnet (Magnex, Abingdon, UK), equipped with high-performance gradients (20 cm ID, 200 mT/m, 260 microseconds rise time) and interfaced to an Avance (Bruker, Ettlingen, Germany) console. A custom-built ^{31}P radiofrequency surface coil (Ø2.5 cm, 68.97 MHz) was used to measure brain pH. Shimming procedure and anatomical imaging were performed using a ^{1}H surface coil (Ø5 cm, 170.28 MHz; Bruker).

Each animal underwent MR sessions at four different stages of the disease: before pump implantation (Ctrl), 1 day after (D1), 3 days after (D3), and 5 days after (D5). For each session, the MR experiment was conducted as follows: scout fast low angle shot (FLASH) images were acquired to position the ^{31}P detection volume ($10 \times 7 \times 8\,mm^3$) in the rat brain. First- and second-order shimming was performed on this volume, leading to a typical ~15 Hz line width on water. Then two ^{31}P spectra were acquired using an optimized point resolved spectroscopy (PRESS) sequence (echo time/repetition time = 8.1/4,000 milliseconds, 1,024 points, 5,900 Hz spectral width, NT = 1,024, acquisition time = 68 minutes). Considering the long acquisition time, a scout image was acquired between the two ^{31}P acquisitions to check for animal position. In case of motion, the voxel of interest was repositioned and shimming procedures were repeated. The two ^{31}P spectra were then phased, corrected from frequency shift and summed. Finally, T2-weighted images optimized to detect cerebral lesions (rapid acquisition with refocused echoes (RARE), echo time/repetition time = 60/3,000 milliseconds, 192 × 192 matrix, 300 μm in-plane resolution) were acquired. The total acquisition time including shimming, ^{31}P spectroscopy and anatomical imaging was ~3 hours.

Processing of Rodent Spectra: All ^{31}P spectra were zero filled to 2,048 points and analyzed using an Advanced Method for Spectral Fitting (AMARES) within jMRUI software (MRUI Project, European Union Program) (Naressi *et al*, 2001). Thirteen ^{31}P multiplets were included in the basis set (Jensen *et al*, 2002), assuming lorentzian line shapes (S = singlet, D = doublet, T = triplet): PE (phosphoethanolamine) (S), Pser (phosphoserine) (S), PC (phosphocholine) (S), DPG (2,3-diphosphoglycerate) (D), Pi (inorganic phosphate) (S), GPE (glycerophosphoethanolamine) (S), GPC (glycerophosphocholine) (S), MP (membrane phospholipids) (S), PCr (phosphocreatine) (S), ATPγ (adenosine triphosphate γ) (D), α ATPα (D) and β ATPβ (T), and NAD (nicotinamide adenine dinucleotides) (S). Resonance frequencies and line widths used as prior knowledge were estimated using the values of T2 and J-coupling constants taken from the literature (Govindaraju *et al*, 2000). Strong constraints were applied to the amplitude (*Amp*) and relative resonance frequencies of double and triple multiplicity metabolites to maintain the structure of the corresponding multiplets: $Amp(\mathrm{DPG})_1 = Amp(\mathrm{DPG})_2$, $Amp(\mathrm{ATP}\alpha)_1 = Amp(\mathrm{ATP}\alpha)_2$, $Amp(\mathrm{ATP}\gamma)_1 = Amp(\mathrm{ATP}\gamma)_2$, $Amp(\mathrm{ATP}\beta)_1 = 0.5 \times Amp(\mathrm{ATP}\beta)_2 = Amp(\mathrm{ATP}\beta)_3$. Relative amplitudes of all phospholipids resonances were estimated from a high signal-to-noise ratio (SNR) spectrum (sum of spectra from the four imaging time points), and empirically set as: $Amp(\mathrm{PSer}) = 0.35 \times Amp(\mathrm{PE})$, $Amp(\mathrm{MP}) = 1.2 \times Amp(\mathrm{GPC})$, $Amp(\mathrm{GPE}) = 0.56 \times Amp(\mathrm{GPC})$. The relative phase of each resonance was calculated from the estimated phase of the PCr peak, assuming a first-order phase of 1.5° per p.p.m.

(corresponding to the delay between excitation and first acquisition point). Soft constraints were applied on the resonance frequencies of all metabolites to allow for pH-induced chemical shift variations. Importantly, no strong constraint was applied to the quantification of the Pi peak. Given the relatively low sensitivity of ^{31}P detection in rodents, ^{31}P spectra were summed over the five animals for each time point (Ctrl, D1, D3, and D5). Indeed, fitting the average spectra minimizes numerical instabilities associated with the fit of noisy data sets (Boumezbeur *et al*, 2004; Henry *et al*, 2002). Then, pH was calculated for the four time points with jMRUI from the chemical shift of Pi relative to PCr. The parameters of Pi–PCr system were set to pK = 6.77, $\delta_{HA} = 3.23$, and $\delta_A = 5.70$ p.p.m. (Petroff and Prichard, 1983).

Cerebral pH in Huntington's Disease Patients

Patients and Control Subjects: The study was conducted on 13 participants: seven HD patients (five males, two females, aged 47 ± 11 years) presenting global brain atrophy, as qualitatively assessed on T1-weighted clinical MR images, and six controls matched for age and sex (four males, two females, aged 43 ± 8 years). The duration of HD since the onset of symptoms was comparable for all seven patients (7 ± 1 years). Patients were recruited in the framework of the MIG-HD (multicentric intracerebral grafting in HD). The protocol was approved by the ethics committee of Henri Mondor Hospital. All subjects gave their written informed consent. They had no psychiatric or neurologic disorders except HD. Table 1 summarizes the characteristics of all patients included in the study (age, gender, body mass index, and number of cytosine-adenine-guanine (CAG) trinucleotide repeats in Huntingtin gene) as well as their UHDRS (Unified Huntington's Disease Rating Scale) clinical scores (Huntington Study Group, 1996). The age and gender of the control subjects are also reported in Table 1.

Nonlocalized ^{31}P Spectroscopy: Human experiments were performed on a whole-body 3 T system (Bruker) equipped with a ^{31}P quadrature birdcage coil (Ø27 cm, 50.7 MHz). Contrary to rodents, the volume of skeletal muscle surrounding the human skull is negligible as compared with the brain volume. For this reason, ^{31}P signal can be localized in the brain by the radiofrequency coil only (Hamakawa *et al*, 2004; Kato *et al*, 1994). The edge of the cylindrical coil was positioned at the level of the upper lip so that the detection volume contained the brain while limiting contamination from masseter, sternocleidomastoid, and trapezius muscles. First-order shimming was performed manually on the ^{31}P signal, leading to a typical ~15 Hz line width on PCr. Spectra were then collected using a pulse-acquire ^{31}P sequence without localization (100 microseconds 90° hard pulse, SW 10k, 1,024 points, repetition time = 7.5 seconds, NT = 28). The total acquisition time including shimming and collection of the pulse-acquire spectra was < 10 minutes.

Processing of Human Spectra: Pulse-acquire ^{31}P spectra of the upper head exhibit the superimposition of metabolite peaks to a broad baseline associated with bone signal (line width ≈ 50 p.p.m.) (McNamara *et al*, 1994), which must be eliminated for valuable quantification of metabolites. To do so, the truncating function of the AMARES package was used, as previously described (Vanhamme *et al*, 1997). Briefly, this function allowed to left shift the free induction decays (FIDs) 12 points (1.2 milliseconds) to eliminate the background signal, quantify the truncated signal, and finally automatically correct the amplitudes and line widths of the estimated components for the truncated points through adjustment of the estimated lorentzian line shapes of all metabolites to the original signal. Spectra quantification and pH calculation were performed as in rodents. However, the higher sensitivity of human ^{31}P acquisitions allowed for individual pH calculation for each human subject. Given the small number of subjects, a Wilcoxon statistic analysis was performed to assess the significance of pH changes between HD and control groups.

Table 1 Characteristics of the seven Huntington's disease (HD) patients and six control subjects included in the study

Patient ID	*Patient 1*	*Patient 2*	*Patient 3*	*Patient 4*	*Patient 5*	*Patient 6*	*Patient 7*
Age (years)	34	53	43	49	33	59	59
Sex	F	M	M	M	M	F	M
BMI	21	24	21	27	19	21	22
Number of CAG repeats	49	45	46	43	54	41	44
UHDRS clinical scores							
Motor score	37	34	72	33	28	27	21
Verbal fluency 1 minute/2 minutes	22/27	34/50	12/21	35/49	12/14	28/37	23/35
Symbol digit	19	22	16	16	28	23	27
Stroop	40/50/23	30/74/31	25/50/19	38/58/20	68/79/34	51/78/23	37/56/33
Behavioral score	20	5	2	4	9	3	18
Functional score	28	28	30	27	28	25	27
Independence scale	80	85	80	100	90	100	80
Total functional capacity	10	11	9	11	11	12	9
Control ID	Control 1	Control 2	Control 3	Control 4	Control 5	Control 6	
	37	44	57	44	35	42	
	M	M	M	F	F	M	

BMI, body mass index; CAG, cytosine-adenine-guanine; UHDRS, Unified Huntington's Disease Rating Scale.

Results

Rodent Model of Huntington's Disease

Animal Physiology and Behavior: Animal behavior was monitored over the protocol duration (5 days) to assess the effects of the 3NP chronic intoxication. At D1 (24 hours after implantation of 3NP-delivering pumps), no obvious toxic effect was visible. However, all 3NP-treated rats showed symptoms of drowsiness, slowness of movement, and general uncoordination at D3. After 5 days, all animals were lying in a recumbent position and showed typical paddling movements of hind limbs, in agreement with previous description of this intoxication model (Bizat *et al*, 2003*a*; Garcia *et al*, 2002; Mittoux *et al*, 2002; Ouary *et al*, 2000).

Measurement of Cerebral pH: Typical ^{31}P spectra collected before 3NP administration and on the third day of 3NP administration are presented in Figure 1. Cerebral pH values are plotted versus time in Figure 2A. An increase in brain pH was detected on the first day of 3NP intoxication as compared with the control value ($pH_{D1} = 7.11 \pm 0.02$ versus $pH_{Ctrl} = 7.08 \pm 0.03$, $P = 0.1$). On the third day of 3NP intoxication, brain pH became significantly higher than the control value ($pH_{D3} = 7.17 \pm 0.02$ versus $pH_{Ctrl} = 7.08 \pm 0.03$, $P < 0.001$). After the onset of striatal lesions on D5, brain pH decreased but remained significantly higher than before 3NP administration ($pH_{D5} = 7.12 \pm 0.02$ versus $pH_{Ctrl} = 7.08 \pm 0.03$, $P = 0.04$).

Correlation with Succinate Dehydrogenase Inhibition: Using a well-characterized 3NP model allowed us to compare changes in brain pH with SDH inhibition previously reported on the exact same model of chronic intoxication: Figure 2A shows the time course of SDH inhibition reported by Bizat *et al* (2003*a*). Comparison with our study showed significant correlation of ^{31}P-measured pH with SDH inhibition ($P < 0.05$).

Detection of Striatal Lesions: Figure 2B shows T2-weighted MRI acquired on the same animal. No major lesion was visible in any animal before D5. In contrast, massive striatal lesions were detected at D5 on the five animals, as shown by strong T2 hypersignal in both striata.

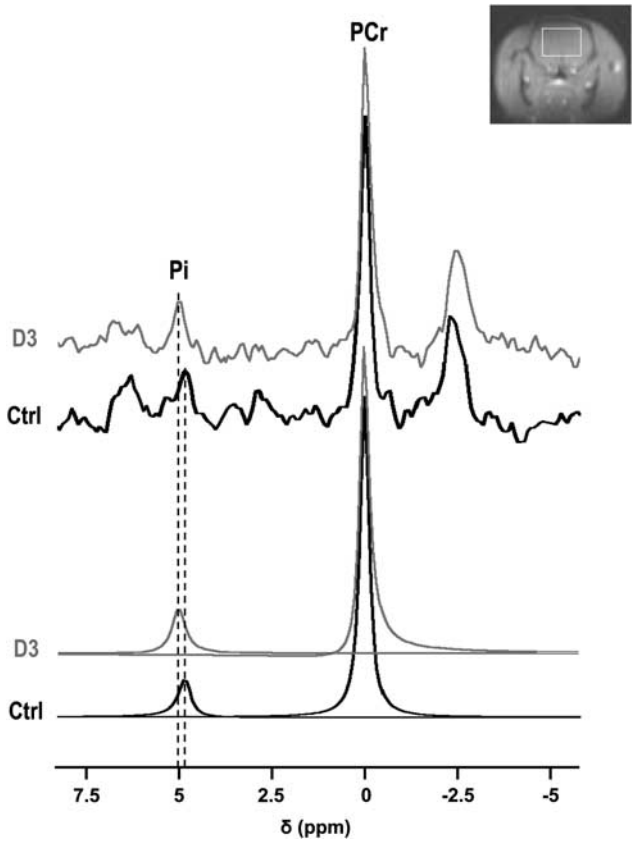

Figure 1 ^{31}P spectra acquired before 3-nitropropionic acid (3NP) administration (Ctrl), and on the third day of 3NP administration (D3). The inorganic phosphate (Pi) peak is shifted toward alkaline chemical shift values (upfield) upon 3NP treatment. The detection volume (white rectangle) is shown on a coronal scout magnetic resonance (MR) image.

Huntington's Disease Patients

Measurement of Cerebral pH: ^{31}P measurement of brain pH was successfully conducted for all HD patients included in the study. Our acquisition procedure made it possible to accurately measure brain pH in < 10 minutes, with a low sensitivity to head motion appropriate for patients suffering from abnormal movements. Typical nonlocalized ^{31}P

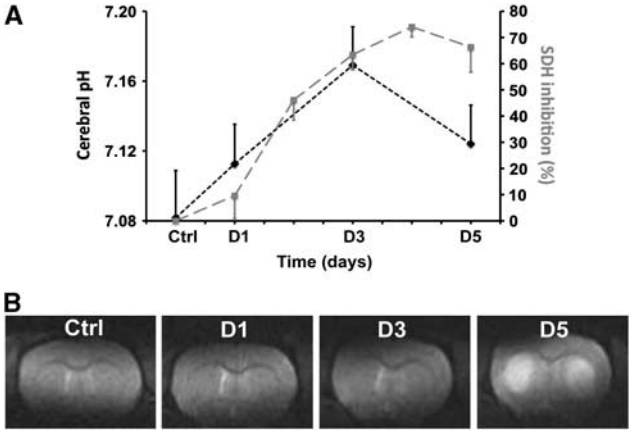

Figure 2 (**A**) Time course of cerebral pH (◆) during the 3-nitropropionic acid (3NP) intoxication protocol showing a significant increase at day 3 (D3), followed by a significant decrease on day 5 (D5). pH changes appear correlated with succinate dehydrogenase (SDH) inhibition (■); (**B**) magnetic resonance imaging (MRI) images acquired in one rat during the intoxication protocol, demonstrating the absence of MRI-visible lesion before D5 and major striatal lesions at D5.

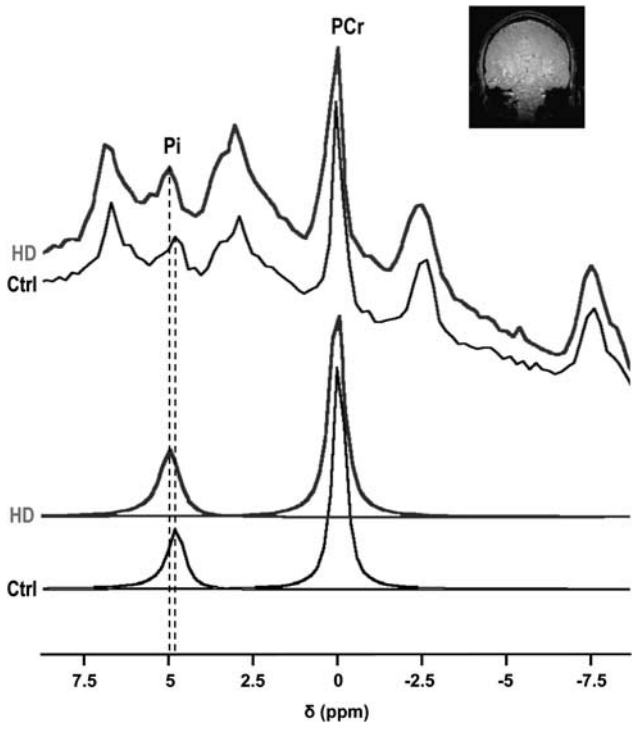

Figure 3 Typical ^{31}P spectra acquired in one Huntington's disease patient (HD) and in one healthy subject (Ctrl), illustrating the inorganic phosphate (Pi) shift toward alkaline values in HD. The detection volume (whole brain) is shown on a coronal scout magnetic resonance imaging (MRI).

spectra acquired in one HD patient and in one healthy subject are shown in Figure 3. The spectra demonstrate upfield Pi shift toward alkaline values in HD. Brain pH was significantly higher in HD than in controls ($pH_{HDpatients} = 7.05 \pm 0.03$ versus $pH_{control} = 7.02 \pm 0.01$, $P = 0.026$). Note that no correlation was found between pH and the number of CAG repeats, likely due to the narrow range of CAG repeats (41 to 54) in the HD group.

Metabolite Concentrations: For controls and HD patients, the relative concentration of each ^{31}P-detected metabolite was calculated as the ratio of metabolite peak area to the sum of all ^{31}P peak areas. No significant difference was observed in metabolite concentrations between HD patients and controls (data not shown).

Discussion

Localization of pH Measurements

All pH values reported in this study are global cerebral values. In the 3NP rodent model, pH measurements were actively localized to the brain using a single voxel PRESS sequence to avoid signal contamination from the surrounding skeletal muscles. Given the negligible amount of muscle tissue surrounding the human skull (Hamakawa *et al*, 2004; Kato *et al*, 1994), the human study was based on nonactively localized pH measurements, the cerebral localization being passively defined by the geometry of the volume coil.

Huntington's disease being characterized by an early striatal neurodegeneration preceding the onset of cognitive and motor symptoms (Harper, 1991), ^{31}P-MRS measurements localized to the striatum would be of high interest. However, one is faced with intrinsic difficulties when trying to perform localized ^{31}P-MRS in HD patients striata. On the technical side, localized ^{31}P-MRS is an intrinsically low sensitivity method. Furthermore, because of the major atrophy of HD patients striata, this structure is of low cellular density. The combination of these methodological and biological limitations make it impossible to obtain localized striatal measurements in experimental conditions compatible with clinical examination of HD neurologic patients, as ^{31}P-MRS low sensitivity combined with striatal low cellular content leads to poor signal-to-noise and strong partial volume effect.

Nonetheless, global brain pH measurements may be a useful indicator of brain energy status in HD. Even though HD is characterized by early striatal neurodegeneration, energy deficits in this pathology have been shown to affect the entire brain, particularly, the cortex and the basal ganglia, and even peripheral organs (Mochel and Haller, 2011; Thibaud *et al*, 2010). As a consequence, the global cerebral pH measured in this study are weighted means of pH values from all cerebral regions, which all are, at least partially, affected by neurodegeneration or energy deficit. In other words, the measurement of whole-brain cerebral pH reflects global energetic deficiency in HD.

Correlation Between pH, Brain Lesion, and Enzymatic Inhibition

The translational study presented here demonstrates significant pH increases in both animal model and HD patients. First of all, the use of a well-characterized animal model made it possible to follow HD progression and to look for parallels between pH changes and development of brain lesions. In all animals, no striatal lesion was detected by T2-weighted MRI at D3, the time point when cerebral pH reached its highest value. In contrast, all rats exhibited bilateral striatal lesions at D5. Therefore, significant changes in cerebral pH can be measured using ^{31}P-MRS before any detection of brain lesion by conventional anatomical imaging. Furthermore, pH changes correlated with the inhibition of the mitochondrial enzyme SDH, showing a regular increase from D1 to D3 followed by a slight decrease. It must be kept in mind that defect in SDH activity—which has been consistently found in several post

mortem biochemical analyses of the HD striatum (Damiano *et al*, 2010)—is a key feature of this disease. As a consequence, ^{31}P-derived pH appears as an early biomarker of neurodegeneration in the animal model, reflecting the metabolic impairment status consecutive to SDH inhibition.

Arguments for Intracellular Neuronal pH Increase

Under normal physiological conditions, a large majority of brain Pi is intracellular, so that MRS measurement of pH is considered as a measure of intracellular pH. One may wonder whether this holds true in HD, knowing that extracellular pH is significantly higher than intracellular pH (7.30 versus 7.05) (Kaila and Bruce, 1998), and that brain atrophy may significantly increase extracellular contribution. Quantitative estimate of intracellular and extracellular contributions to the Pi peak (Veech *et al*, 1979) shows that intracellular contribution under physiological conditions is $\sim$40 times as high as extracellular contribution: intracellular Pi concentration ($\sim$2.5 mmol/L) is five times as high as extracellular concentration ($\sim$0.5 mmol/L) (Luyten *et al*, 1989; Veech *et al*, 1979) and intracellular volume is eight times as high as extracellular volume in the brain (Mascalchi *et al*, 2004). Therefore, extracellular Pi could contribute to the measured pH increase only in case of strongly increased extracellular volume. This possibility is not supported by currently available data: the relaxation time T2, which is highly sensitive to extracellular volume, does not exhibit any change in our rats during pH increase (first 3 days of 3NP intoxication). In addition, no histological alteration was observed in the rat brain at the same stage of intoxication (Bizat *et al*, 2003*a*). Human data also show that HD patients exhibit T2 values, which are similar or shorter than healthy subjects (Vymazal *et al*, 2007). Consequently, pH values measured in our study are likely to represent intracellular pH, under physiological as well as under pathological conditions. Recent *in vivo* MRS data suggest that a large majority of brain Pi is located in neurons as opposed to glial cells, based on the fact that Pi is in a compartment where oxidative metabolism strongly dominates glycolytic metabolism (Chaumeil *et al*, 2009; Lei *et al*, 2003). Altogether, these observations allow us to interpret our results as an increase in neuronal pH in HD.

Interpretation of pH Changes

Potential Role of Na+/H+ Exchanger: Cerebral alkalosis has been reported in several other brain diseases such as transient ischemia (Kogure *et al*, 1980; Mabe *et al*, 1983), acute ischemic stroke (Chopp *et al*, 1990), chronic cerebral infarction (Hugg *et al*, 1992; Sappey-Marinier *et al*, 1992), hypoxic encephalopathy (Mitsufuji *et al*, 1995), and neonatal encephalopathy (Robertson *et al*, 2002). The most common explanation for alkaline pHi includes the activation of the electroneutral Na+/H+ exchanger: Na+ influx into the cell induces the efflux of H+ to maintain electroneutrality. Triggers of Na+/H+ antiporter activation are still investigated, as this transporter is regulated by several extracellular factors such as hormones, growth factors, and cytokines. Interestingly, brain pHi was also positively correlated with brain tissue lactate levels in most studies. One hypothesis is that systemic accumulation of sodium lactate would be the trigger to the intracellular alkaline shift through a compensatory mechanism involving Na+/H+ exchangers. Another hypothesis in that astrocytes alkalinization could increase the glycolitic rate through the pH-dependent activation of phosphofructokinease, inducing in turn an excess of lactate pumped out of the cellular compartment. Decrease in the PCr/Pi ratios reported in hypoxia supports the hypothesis of an increased glycolysis. In the case of HD, increased lactate levels have been reported by Jenkins *et al* (1993, 1998) but no changes in ^{31}P-containing metabolites were found in our study. Further studies will therefore be required to establish whether lactate activated Na+/H+ antiporter significantly contributes to pH changes in HD.

Correlation with Biochemical Events Associated with 3-Nitropropionic Acid Degeneration: The 3NP model used here has been previously characterized in our laboratory and by other groups worldwide (Bizat *et al*, 2003*a*, *b*; Brouillet *et al*, 2005). One important characteristic of this 3NP model is that all animals respond homogenously to the toxic effects of the neurotoxin. Therefore, pH changes measured in our study can be interpreted with regard to biochemical events previously reported for this model: from the beginning of 3NP treatment to D3, no histological brain lesion was observed. However, on day 3, biochemical evaluation of the striatum in 3NP-treated animals showed that cytochrome C was released from mitochondria to the cytoplasm, reflecting mitochondrial impairment in particular loss of mitochondria membrane potential in the striatum. Later on day 4, caspase-9 was transiently found in its active form as seen using enzymatic, biochemical, and immunohistochemical analysis (Bizat *et al*, 2003*a*, *b*). Activation of caspase-9 is an ATP-dependent process, so that at day 3 ATP levels are likely to be maintained in the striatum of 3NP-treated rats. On day 4, deregulation of Ca^{2+} homeostasis, resulting from mitochondrial dysfunction, produced massive activation of the protease calpain leading to cell demise. At day 4 to day 4.5, histological lesions appeared in the striatum (Bizat *et al*, 2003*a*). These data confirm, in addition to our MRI data showing no T2 change in the striata before D5, that pH increase precedes striatal lesions and might be concurrent to early mitochondrial dysfunction associated with maintained ATP level.

Structure of Inorganic Phosphate Resonance: Increased pH has recently been observed in muscle disease using the same ^{31}P-MRS approach (Thibaud *et al*, 2010). The sensitivity of ^{31}P detection being much higher in skeletal muscle than in the brain, the authors observed that the Pi peak was not simply shifted toward alkaline values, but that a second Pi peak appeared nearby the 'physiological' Pi peak ($\sim$0.3 p.p.m. upfield) under pathological conditions. This second Pi peak was ascribed to a pool of suffering cells that could not maintain proper ionic homeostasis. Given the detection sensitivity and spectral resolution of our brain studies, it is very likely that such a peak would not be discriminated from the 'physiological' Pi peak on our data, resulting in an enlarged combined Pi peak which maximum intensity is shifted toward alkaline chemical shift.

Conclusion

In conclusion, the translational approach used here shows that neuronal pH (1) is increased in an animal model of HD as well as in HD patients, (2) correlates with enzymatic impairment, and (3) increases before histological and MRI-visible brain lesion in rodents. Given the increasing availability of ^{31}P-MRS on clinical MR scanners, these results make intracellular pH a promising biomarker for HD. Longitudinal measurements on the same patients will be needed to determine whether ^{31}P-derived pH is a reliable biomarker of disease progression in the individual patient.

Fundamental studies are also required to better characterize the structure of the Pi peak observed on the ^{31}P spectrum under pathological conditions. Given the relatively low sensitivity and spectral resolution at 3 and 4 T, our study does not rule out the possibility of an additional Pi peak appearing upfield under degeneration, as reported in muscle disease (Thibaud *et al*, 2010). *In vivo* studies at higher magnetic field will be necessary to address this issue.

Finally, alternative approaches are available for *in vivo* pH measurement, based on PE detection (Corbett *et al*, 1987; Petroff *et al*, 1985) or on nucleoside triphosphates detection (Williams and Smith, 1995). Although the sensitivity of our low-field study did not make it possible to implement these approaches, further high-field studies will be of major interest to confirm and help interpret our results.

Acknowledgements

The MIG-HD trial is granted through two PHRC AOM00139 and AOM 04021 from the DRCD (Assistance Publique-Hôpitaux de Paris) and the support of the AFM. The management center involves ACB-L (principal investigator), S Palfi, P Remy, M Peschanski, P Hantraye, JP Lefaucheur, D Challine, and P Maison. CROs were AR and D Schmitz. The sites PI are ACB-L, S Palfi (Créteil), P Krystkowiak, S Blond (Lille), JF Démonet, Y Lazorthes (Toulouse), CV, P Menei (Angers), P Damier, Y Lajat (Nantes), F Supiot, M Levivier (Bruxelles).

Disclosure/conflict of interest

The authors declare no conflict of interest.

References

Albers MJ, Krieger MD, Gonzalez-Gomez I, Gilles FH, McComb JG, Nelson Jr MD, Bluml S (2005) Proton-decoupled 31P MRS in untreated pediatric brain tumors. *Magn Reson Med* 53:22–9

Beal MF (2005) Mitochondria take center stage in aging and neurodegeneration. *Ann Neurol* 58:495–505

Bizat N, Hermel JM, Boyer F, Jacquard C, Creminon C, Ouary S, Escartin C, Hantraye P, Kajewski S, Brouillet E (2003*a*) Calpain is a major cell death effector in selective striatal degeneration induced *in vivo* by 3-nitropropionate: implications for Huntington's disease. *J Neurosci* 23:5020–30

Bizat N, Hermel JM, Humbert S, Jacquard C, Creminon C, Escartin C, Saudou F, Krajewski S, Hantraye P, Brouillet E (2003*b*) *In vivo* calpain/caspase cross-talk during 3-nitropropionic acid-induced striatal degeneration: implication of a calpain-mediated cleavage of active caspase-3. *J Biol Chem* 278:43245–53

Boumezbeur F, Besret L, Valette J, Gregoire MC, Delzescaux T, Maroy R, Vaufrey F, Gervais P, Hantraye P, Bloch G, Lebon V (2005) Glycolysis versus TCA cycle in the primate brain as measured by combining 18F-FDG PET and 13C-NMR. *J Cereb Blood Flow Metab* 25:1418–23

Boumezbeur F, Besret L, Valette J, Vaufrey F, Henry PG, Slavov V, Giacomini E, Hantraye P, Bloch G, Lebon V (2004) NMR measurement of brain oxidative metabolism in monkeys using 13C-labeled glucose without a 13C radiofrequency channel. *Magn Reson Med* 52:33–40

Brouillet E, Conde F, Beal MF, Hantraye P (1999) Replicating Huntington's disease phenotype in experimental animals. *Prog Neurobiol* 59:427–68

Brouillet E, Jacquard C, Bizat N, Blum D (2005) 3-Nitropropionic acid: a mitochondrial toxin to uncover physiopathological mechanisms underlying striatal degeneration in Huntington's disease. *J Neurochem* 95:1521–40

Chaumeil MM, Valette J, Guillermier M, Brouillet E, Boumezbeur F, Herard AS, Bloch G, Hantraye P, Lebon V (2009) Multimodal neuroimaging provides a highly consistent picture of energy metabolism, validating 31P MRS for measuring brain ATP synthesis. *Proc Natl Acad Sci USA* 106:3988–93

Chopp M, Vande Linde AM, Chen H, Knight R, Helpern JA, Welch KM (1990) Chronic cerebral intracellular alkalosis following forebrain ischemic insult in rats. *Stroke* 21:463–6

Corbett RJ, Nunnally RL, Giovanella BC, Antich PP (1987) Characterization of the 31P nuclear magnetic resonance spectrum from human melanoma tumors implanted in nude mice. *Cancer Res* 47:5065–9

Damiano M, Galvan L, Deglon N, Brouillet E (2010) Mitochondria in Huntington's disease. *Biochim Biophys Acta* 1802:52–61

Dautry C, Vaufrey F, Brouillet E, Bizat N, Henry PG, Conde F, Bloch G, Hantraye P (2000) Early N-acetylaspartate depletion is a marker of neuronal dysfunction in rats and primates chronically treated with the mitochondrial toxin 3-nitropropionic acid. *J Cereb Blood Flow Metab* 20:789–99

Garcia M, Vanhoutte P, Pages C, Besson MJ, Brouillet E, Caboche J (2002) The mitochondrial toxin 3-nitropropionic acid induces striatal neurodegeneration via a c-Jun N-terminal kinase/c-Jun module. *J Neurosci* 22:2174–84

Gerweck LE, Seetharaman K (1996) Cellular pH gradient in tumor versus normal tissue: potential exploitation for the treatment of cancer. *Cancer Res* 56:1194–8

Govindaraju V, Young K, Maudsley AA (2000) Proton NMR chemical shifts and coupling constants for brain metabolites. *NMR Biomed* 13:129–53

Hamakawa H, Murashita J, Yamada N, Inubushi T, Kato N, Kato T (2004) Reduced intracellular pH in the basal ganglia and whole brain measured by 31P-MRS in bipolar disorder. *Psychiatry Clin Neurosci* 58:82–8

Hamilton G, Mathur R, Allsop JM, Forton DM, Dhanjal NS, Shaw RJ, Taylor-Robinson SD (2003) Changes in brain intracellular pH and membrane phospholipids on oxygen therapy in hypoxic patients with chronic obstructive pulmonary disease. *Metab Brain Dis* 18:95–109

Harper PS (1991) *Huntington's Disease*. Saunders: London

Henry PG, Lebon V, Vaufrey F, Brouillet E, Hantraye P, Bloch G (2002) Decreased TCA cycle rate in the rat brain after acute 3-NP treatment measured by *in vivo* 1H-[13C] NMR spectroscopy. *J Neurochem* 82:857–66

Hoang TQ, Bluml S, Dubowitz DJ, Moats R, Kopyov O, Jacques D, Ross BD (1998) Quantitative proton-decoupled 31P MRS and 1H MRS in the evaluation of Huntington's and Parkinson's diseases. *Neurology* 50:1033–40

Hugg JW, Duijn JH, Matson GB, Maudsley AA, Tsuruda JS, Gelinas DF, Weiner MW (1992) Elevated lactate and alkalosis in chronic human brain infarction observed by 1H and 31P MR spectroscopic imaging. *J Cereb Blood Flow Metab* 12:734–44

Jenkins BG, Koroshetz WJ, Beal MF, Rosen BR (1993) Evidence for impairment of energy metabolism *in vivo* in Huntington's disease using localized 1H NMR spectroscopy. *Neurology* 43:2689–95

Jenkins BG, Rosas HD, Chen YC, Makabe T, Myers R, MacDonald M, Rosen BR, Beal MF, Koroshetz WJ (1998) 1H NMR spectroscopy studies of Huntington's disease: correlations with CAG repeat numbers. *Neurology* 50:1357–65

Jensen JE, Daniels M, Haws C, Bolo NR, Lyoo IK, Yoon SJ, Cohen BM, Stoll AL, Rusche JR, Renshaw PF (2008) Triacetyluridine (TAU) decreases depressive symptoms and increases brain pH in bipolar patients. *Exp Clin Psychopharmacol* 16:199–206

Jensen JE, Drost DJ, Menon RS, Williamson PC (2002) *In vivo* brain (31)P-MRS: measuring the phospholipid resonances at 4 Tesla from small voxels. *NMR Biomed* 15:338–47

Kaila KR, Bruce R (1998) *pH and Brain Function*. Wiley-Liss: England

Kato T, Shioiri T, Murashita J, Hamakawa H, Inubushi T, Takahashi S (1994) Phosphorus-31 magnetic resonance spectroscopy and ventricular enlargement in bipolar disorder. *Psychiatry Res* 55:41–50

Kogure K, Busto R, Schwartzman RJ, Scheinberg P (1980) The dissociation of cerebral blood flow, metabolism, and function in the early stages of developing cerebral infarction. *Ann Neurol* 8:278–90

Kuhl DE, Phelps ME, Markham CH, Metter EJ, Riege WH, Winter J (1982) Cerebral metabolism and atrophy in Huntington's disease determined by 18FDG and computed tomographic scan. *Ann Neurol* 12:425–34

Lei H, Ugurbil K, Chen W (2003) Measurement of unidirectional Pi to ATP flux in human visual cortex at 7 T by using *in vivo* 31P magnetic resonance spectroscopy. *Proc Natl Acad Sci USA* 100:14409–14

Luyten PR, Bruntink G, Sloff FM, Vermeulen JW, van der Heijden JI, den Hollander JA, Heerschap A (1989) Broadband proton decoupling in human 31P NMR spectroscopy. *NMR Biomed* 1:177–83

Mabe H, Blomqvist P, Siesjo BK (1983) Intracellular pH in the brain following transient ischemia. *J Cereb Blood Flow Metab* 3:109–14

Mascalchi M, Lolli F, Della Nave R, Tessa C, Petralli R, Gavazzi C, Politi LS, Macucci M, Filippi M, Piacentini S (2004) Huntington disease: volumetric, diffusion-weighted, and magnetization transfer MR imaging of brain. *Radiology* 232:867–73

McNamara R, Arias-Mendoza F, Brown TR (1994) Investigation of broad resonances in 31P NMR spectra of the human brain *in vivo*. *NMR Biomed* 7:237–42

Mitsufuji N, Yoshioka H, Tominaga M, Okano S, Nishiki T, Sawada T (1995) Intracellular alkalosis during hypoxia in newborn mouse brain in the presence of systemic acidosis: a phosphorus magnetic resonance spectroscopic study. *Brain Dev* 17:256–60

Mittoux V, Ouary S, Monville C, Lisovoski F, Poyot T, Conde F, Escartin C, Robichon R, Brouillet E, Peschanski M, Hantraye P (2002) Corticostriatopallidal neuroprotection by adenovirus-mediated ciliary neurotrophic factor gene transfer in a rat model of progressive striatal degeneration. *J Neurosci* 22:4478–86

Mochel F, Haller RG (2011) Energy deficit in Huntington disease: why it matters. *J Clin Invest* 121:493–9

Naressi A, Couturier C, Castang I, de Beer R, Graveron-Demilly D (2001) Java-based graphical user interface for MRUI, a software package for quantitation of *in vivo*/medical magnetic resonance spectroscopy signals. *Comput Biol Med* 31:269–86

Ouary S, Bizat N, Altairac S, Menetrat H, Mittoux V, Conde F, Hantraye P, Brouillet E (2000) Major strain differences in response to chronic systemic administration of the mitochondrial toxin 3-nitropropionic acid in rats: implications for neuroprotection studies. *Neuroscience* 97:521–30

Petroff OA, Prichard JW (1983) Cerebral pH by NMR. *Lancet* 2:105–6

Petroff OA, Prichard JW, Behar KL, Alger JR, den Hollander JA, Shulman RG (1985) Cerebral intracellular pH by 31P nuclear magnetic resonance spectroscopy. *Neurology* 35:781–8

Powers WJ, Videen TO, Markham J, McGee-Minnich L, Antenor-Dorsey JV, Hershey T, Perlmutter JS (2007) Selective defect of *in vivo* glycolysis in early Huntington's disease striatum. *Proc Natl Acad Sci USA* 104:2945–9

Rango M, Bonifati C, Bresolin N (2006) Parkinson's disease and brain mitochondrial dysfunction: a functional phosphorus magnetic resonance spectroscopy study. *J Cereb Blood Flow Metab* 26:283–90

Robertson NJ, Cowan FM, Cox IJ, Edwards AD (2002) Brain alkaline intracellular pH after neonatal encephalopathy. *Ann Neurol* 52:732–42

Sappey-Marinier D, Hubesch B, Matson GB, Weiner MW (1992) Decreased phosphorus metabolite concentrations

and alkalosis in chronic cerebral infarction. *Radiology* 182:29–34

Thibaud JL, Wary C, Naulet T, Duteil S, Monnet A, Blot S, Carlier PG (2010) Two pools of inorganic phosphate in canine model of DMD evidenced by phosphorus NMR spectroscopy. In: *XII ICNMD*, Naples. *Acta Myologica* 29:225

Huntington Study Group (1996) Unified Huntington's disease rating scale: reliability and consistency. *Mov Disord* 11:136–42

van der Grond J, Gerson JR, Laxer KD, Hugg JW, Matson GB, Weiner MW (1998) Regional distribution of interictal 31P metabolic changes in patients with temporal lobe epilepsy. *Epilepsia* 39:527–36

Vanhamme L, van den Boogaart A, Van Huffel S (1997) Improved method for accurate and efficient quantification of MRS data with use of prior knowledge. *J Magn Reson* 129:35–43

Veech RL, Lawson JW, Cornell NW, Krebs HA (1979) Cytosolic phosphorylation potential. *J Biol Chem* 254:6538–47

Vymazal J, Klempir J, Jech R, Zidovska J, Syka M, Ruzicka E, Roth J (2007) MR relaxometry in Huntington's disease: correlation between imaging, genetic and clinical parameters. *J Neurol Sci* 263:20–5

Welch KM, Levine SR, Martin G, Ordidge R, Vande Linde AM, Helpern JA (1992) Magnetic resonance spectroscopy in cerebral ischemia. *Neurol Clin* 10:1–29

Williams GD, Smith MB (1995) Application of the accurate assessment of intracellular magnesium and pH from the 31P shifts of ATP to cerebral hypoxia-ischemia in neonatal rat. *Magn Reson Med* 33:853–7